

# Effects of the structure of Ce–Cu catalysts on the catalytic combustion of toluene in air

Guilin Zhou\*, Hai Lan, Xiaoqing Yang, Qingxiang Du, Hongmei Xie, Min Fu

*Key Laboratory of Catalysis Science and Technology of Chongqing Education Commission, Department of Chemistry and Chemical Engineering, Chongqing Technology and Business University, Chongqing 400067, China*

Received 1 October 2012; received in revised form 11 October 2012; accepted 12 October 2012

Available online 23 October 2012

## Abstract

Ce–Cu composite oxide catalysts were prepared by a hard-template method (CeCu-HT) and a complex method (CeCu-CA). The prepared Ce–Cu composite oxide catalysts were characterized by X-ray diffraction (XRD), transmission electron microscopy (TEM), and Brunauer–Emmett–Teller (BET) analyses. The catalytic properties of the prepared Ce–Cu composite oxide catalysts were also investigated by the catalytic combustion of toluene in air. XRD results showed that the synthesized Ce–Cu composite oxide catalysts had different phase components and crystallinities but similar  $\text{CeO}_2$ –CuO solid solution phases. Low-angle XRD, TEM, and BET results indicated that the prepared CeCu-HT catalyst had a developed ordered mesoporous structure and a large specific surface area of  $206.1 \text{ m}^2 \text{ g}^{-1}$ . Toluene catalytic combustion results indicated that the CeCu-HT catalyst had higher toluene catalytic combustion activity in air than the CeCu-CA catalyst. The minimum reaction temperature at which toluene conversion exceeded 90% for toluene catalytic combustion on the CeCu-HT catalyst was  $225^\circ\text{C}$ . The toluene catalytic combustion conversion on the CeCu-HT catalyst at  $240^\circ\text{C}$  exceeded 99.3% with decreased toluene concentration in air to below 70 ppm. On the other hand, the toluene catalytic combustion conversion on the CeCu-CA catalyst was only 92% even when the reaction temperature reached  $280^\circ\text{C}$ . The differences between the toluene catalytic combustion performances of the Ce–Cu composite oxide catalysts prepared by different methods can be attributed to their discrepant compositions and structures.

Crown Copyright © 2012 Published by Elsevier Ltd and Techna Group S.r.l. All rights reserved.

**Keywords:** Ce–Cu composite oxide catalyst; Ordered mesoporous structure; Hard-template method; Complex method

## 1. Introduction

Volatile organic compounds (VOCs) are major components of air pollutants that exist as a wide variety of species with complex compositions. These compounds can significantly harm human health and the environment. Phenyl compounds (e.g., benzene, toluene, xylene, ethylbenzene, etc.) are an important type of VOCs. These stable compounds are extensively applied in different fields, such as the petrochemical, motor fuel, paint, plastic, medical, steel, and detergent industries [1]. These phenyl compounds exhibit high carcinogenicity and toxicity to the

central nervous system, and are thus gaining considerable attention worldwide [2,3]. Many countries have established atmospheric quality standards for benzene, toluene, ethylbenzene, and xylene. For example, on December 1, 2000, the European Union set the average concentration limit for benzene in air as  $5 \mu\text{g m}^{-3}$ . On January 1, 2006, the value was changed to  $1 \mu\text{g m}^{-3}$ . According to the World Health Organization, the average exposure concentration limit for toluene in the atmosphere is  $8.21 \mu\text{g m}^{-3}$  [3].

The treatment methods of phenyl compounds are generally divided into two categories: a recovery method that uses nondisruptive technology, and a method that uses destructive technology. The latter generally involves the use of chemical or biological techniques to transform phenyl compounds into carbon dioxide, water, and other nontoxic or less toxic compounds. The treatment techniques include

\*Corresponding author. Tel.: +86 23 62769076;  
fax: +86 23 62769785 605.

E-mail address: [upczguilin@sohu.com](mailto:upczguilin@sohu.com) (G. Zhou).

direct combustion, catalytic combustion, biodegradation, plasma oxidation, and photocatalytic oxidation. Among these techniques, catalytic combustion, which is used to treat low-concentration phenyl compounds, requires a temperature that is far below that required for direct combustion. Catalytic combustion, which has high purification efficiency and low energy consumption, does not generate secondary pollution. Thus, this method is considered as one of the most effective treatment methods for the elimination of phenyl compounds from air [4]. The catalytic combustion technology used to treat phenyl compounds in air has become a research hotspot in environmental catalysis and has thus been extensively studied. For the catalytic combustion of phenyl compounds, the core issue is the design and development of catalytic materials. In recent years, researchers have focused on noble metal catalysts [5–9]. These noble catalysts exhibit high activities for the catalytic combustion of low-concentration VOCs in the atmosphere. However, these catalysts are expensive, have limited availability, and have low  $\text{CO}_2$  selectivity at the reaction temperatures. Consequently, transition metal catalysts are attracting increasing attention because of their low cost and high activity for the catalytic combustion elimination of VOCs in air [10–12]. Transition metal oxides are functional materials that have been extensively studied in the field of material science. In catalysis, composite metal oxide catalysts exhibit higher catalytic performance than single metal-oxide catalysts.

Transition metal oxide catalysts, which are synthesized by conventional preparation methods, can only weakly adsorb and activate reactant molecules because of their small specific surface area ( $< 30 \text{ m}^2 \text{ g}^{-1}$ ), low porosity, and irregular pore size distribution. With the rapid development of mesoporous materials, studies on the synthesis of mesoporous metal oxide catalysts and their catalytic performances are progressing because of the large specific surface area and developed porous structure of these catalysts. Mesoporous single metal-oxide catalysts have been prepared and successfully used in CO catalytic oxidation, [13–15]. However, reports on the catalytic elimination of phenyl compounds from air using composite metal oxide mesoporous catalysts are limited. Therefore, research on mesoporous or ordered mesoporous composite metal-oxide catalysts for the catalytic combustion of phenyl compounds has important implications for mesoporous catalysts, phenyl compounds catalytic elimination, and environmental protection.

This study aims to synthesize Ce–Cu composite oxide catalysts with different structural properties. The synthesized Ce–Cu composite oxide catalysts were used to catalyze the elimination of toluene from air. The performances of the Ce–Cu composite oxide catalysts on the catalytic elimination of toluene were examined. The prepared Ce–Cu composite oxide catalysts were characterized by X-ray diffraction (XRD), transmission electron microscopy (TEM), and Brunauer–Emmett–Teller (BET) analyses.

## 2. Experimental

### 2.1. Catalyst preparation

In a typical synthesis of mesoporous Ce–Cu oxide catalyst by the hard-template method, 1.0 g each of  $\text{Ce}(\text{NO}_3)_3 \cdot 6\text{H}_2\text{O}$  and  $\text{Cu}(\text{NO}_3)_2 \cdot 6\text{H}_2\text{O}$  ( $n_{\text{Ce}}/n_{\text{Cu}}$  mole ratio = 3.0) was dissolved in 20 mL of ethanol. KIT-6 mesoporous silica was then added. The silica template was prepared according to the procedure described by Ryoo et al. [16]. The mixture was stirred at room temperature until a dry powder was obtained. The powder was then slowly heated to  $400^\circ\text{C}$  and calcined at that temperature for 2.0 h. The impregnation procedure was repeated, followed by calcination at  $500^\circ\text{C}$  for 3 h. The resulting samples were treated three times with 2 M NaOH to remove the silica template. Afterwards, the samples were centrifuged, washed several times with water and ethanol, and then dried at  $100^\circ\text{C}$  in air. The obtained product was designated as CeCu-HT.

In a typical complex-method synthesis of Ce–Cu oxide catalyst,  $\text{Cu}(\text{NO}_3)_2 \cdot 6\text{H}_2\text{O}$ ,  $\text{Ce}(\text{NH}_4)_2(\text{NO}_3)_6$ , and citric acid (CA) ( $n_{\text{Ce}}/n_{\text{Cu}}$  molar ratio = 3.0;  $n_{\text{CA}}/n_{(\text{Ce}+\text{Cu})}$  molar ratio = 1.8) were dissolved in a certain amount of deionized water. The mixture was then stirred at  $80^\circ\text{C}$  until the deionized water completely evaporated. Afterwards, the sample was dried in an oven at  $100^\circ\text{C}$  for 10 h, slowly heated to  $550^\circ\text{C}$ , and calcined at that temperature for 3 h. The CuO–CeO<sub>2</sub> composite oxide catalyst was then obtained and designated as CeCu-CA.

### 2.2. Catalyst characterization

#### 2.2.1. XRD characterization

X-ray diffraction (XRD) patterns were recorded on a Rigaku D/Max-2500/PC diffractometer with a rotating anode using Ni filtered Cu-K $\alpha$  (as radiation source ( $\lambda = 0.15418 \text{ nm}$ )) radiation at 40 kV of a tube voltage and 200 mA of a tube current. The data of  $2\theta$  from  $20^\circ$  to  $80^\circ$  range were collected with the step size of  $0.02^\circ$  at the rate of  $5^\circ \text{ min}^{-1}$ .

#### 2.2.2. TEM analysis

Transmission electron microscopy (TEM) was performed using a Tecnai G<sup>2</sup> Spirit microscope operating with an acceleration voltage of 120 kV. For the TEM measurement, the samples were prepared by ultrasonication in ethanol, evaporating a drop of the resultant suspension onto a carbon-coated copper grid.

#### 2.2.3. BET characterization

Adsorption and desorption isotherms were collected on Autosorb-6 at 77 K. Prior to the measurement, all samples were degassed at 473 K until a stable vacuum of ca. 5 m Torr was reached. The specific surface area was assessed using the Brunauer–Emmett–Teller (BET) method from adsorption data in a relative pressure range from 0.06 to 0.10. The total

pore volume,  $V_t$ , was assessed from the adsorbed amount of nitrogen at a relative pressure of 0.99 by converting it to the corresponding volume of liquid adsorbate.

### 2.3. Catalytic activity measurement

Catalytic tests of all catalysts were carried out in a continuous flow fixed-bed quartz tubular reactor (i.d. 6 mm) under atmospheric pressure. The quartz tube reactor containing 50 mg catalyst was placed inside a tubular furnace. The air was passed downward through the reactor containing the catalyst bed, while electronic mass flow controller (D07-7A/ZM, China) was used to control air flow rate. The feed gas was obtained by bubbling air through a saturator, which contains toluene in liquid phase, kept at 0 °C to achieve the feed gas mixture consisting of gaseous toluene (1.0 vol.%) and the feed gas was led over the catalysts at a flow rate of 55 mL min<sup>-1</sup>, equivalent to a gas mass space velocity of 66,000 mL g<sup>-1</sup> h<sup>-1</sup>. Catalytic activity tests were performed at temperature range of 180–270 °C, which was measured using a thermocouple projecting into the catalyst bed. The reaction temperature was monitored by a temperature programmable controller (ÜGU, model 708P, China) at a heating rate of 2 °C min<sup>-1</sup> until given temperature. Before each test, the catalyst bed was heated to the preconcentrated temperature point at a heating rate of 10 °C min<sup>-1</sup>, and then the feed gas was switched to the catalyst bed and stabilized for 120 min to recording the date for the effluent gas interval 5 min. The quantity of toluene in the feed gas and reaction products gas were monitored by using on-line gas chromatograph (GC 6890II), equipped with a FID.

## 3. Results and discussion

### 3.1. XRD characterization

The XRD patterns of the CeCu-CA and CeCu-HT catalysts are shown in Fig. 1. In the XRD pattern of the CeCu-CA catalyst, eight intense and sharp diffraction peaks appear at 28.56°, 33.12°, 47.46°, 56.32°, 59.14°, 69.44°, 76.66°, and 79.14°, which are associated with the fluorite-like structure of the CeO<sub>2</sub> crystalline phase [17]. At the same time, two relatively weak diffraction peaks of the CuO crystalline phase can be observed at 35.54° and 38.72° [18]. However, in the XRD pattern of the CeCu-HT catalyst, four weak, broad diffraction peaks appear at 28.56°, 33.12°, 47.46°, and 56.32°, which are characteristic of the CeO<sub>2</sub> crystalline phase with a fluorite-like structure. When  $2\theta$  exceeds 60°, the diffraction peaks of the CeO<sub>2</sub> crystalline phase almost disappear corresponding to those in the pattern of the CeCu-CA catalyst. The XRD peaks corresponding to the CuO crystalline phase are not observed in the XRD pattern of the CeCu-HT catalyst.

Different CuO phases are known to exist in CuO–CeO<sub>2</sub> catalysts. For example, Cu<sup>2+</sup> species enter the CeO<sub>2</sub> lattice to form a solid solution. Well-dispersed CuO species and

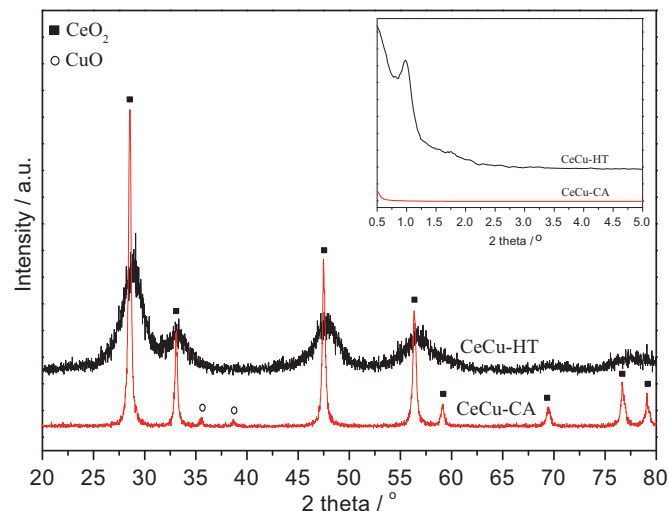


Fig. 1. XRD patterns of CeCu-HT and CeCu-CA catalysts.

CuO–CeO<sub>2</sub> solid solution can also coexist in a catalyst system [19]. As aforementioned, Ce and Cu species in the CeCu-CA catalyst system mainly exist in the crystalline phase of their normal metal oxide (CuO and CeO<sub>2</sub>). However, the CuO–CeO<sub>2</sub> solid solution is obtained because of the dissolution of a large amount of CuO species in the CeO<sub>2</sub> lattice. Only a few highly dispersive CuO crystalline particles are found on the surface of the CuO–CeO<sub>2</sub> catalyst compared with the CeCu-CA catalyst. In the CeCu-HT catalyst system, the XRD peaks of other crystalline phase are not significant except for the weak and broad peaks of the CeO<sub>2</sub> crystalline phase. These results indicate that the CuO species may be completely dissolved in the CeO<sub>2</sub> lattice to destroy the integrated CeO<sub>2</sub> lattice, or that the CuO and CeO<sub>2</sub> crystalline phases exhibit high dispersion in this catalyst system. The “embedded-model” solid solution, also called the Cu–Ce–O composite oxide system, can be formed by “oxide–oxide” interactions in the CuO–CeO<sub>2</sub> solid solution catalyst system [19]. The results imply that CuO and CeO<sub>2</sub> species in the CeCu-HT catalyst system do not exist in the form of simple metal oxides but in the form of Cu–Ce–O composite oxides. In the CeCu-HT catalyst system, the Ce–O and Cu–O bonds are weakened because of the strong interaction between CuO and CeO<sub>2</sub>. These weak metal–oxygen bonds can easily crack to produce active oxygen species. Therefore, the catalyst composition and active component distribution can be improved using different preparation methods. The change in the chemical bonds can radically affect the performance of the composite metal oxide catalysts.

The low-angle XRD peak of the CeCu-CA catalyst, which shows in Fig. 1 illustration, was not be observed at the 0.5° to 5.0° range. However, the low-angle XRD of the CeCu-HT catalyst has a sharp intense peak at  $2\theta=0.98^\circ$ , which corresponds to the (2 1 1) plane. According to previous reports [20], the prepared CeCu-HT catalyst has an ordered mesoporous structure.

### 3.2. TEM analysis

The TEM images of the prepared CeCu-HT and CeCu-CA catalysts are shown in Fig. 2. The prepared CeCu-HT catalyst exhibits a developed mesoporous structure with a pore size of approximately 5–6 nm. On the other hand, the prepared CeCu-CA catalyst exhibits an aggregated structure with a distinct particle size and shape. The particle size diameter ranges from 50 nm to 250 nm.

The hard template KIT-6 reportedly displays a three-dimensional ordered mesoporous structure [16]. Fig. 2 shows that the CeCu-HT catalyst, which was prepared using KIT-6 as a hard template, can be a very effective replica of the KIT-6 structure to form an ordered mesoporous structure. The result is consistent with the low-angle XRD analysis. This structure of KIT-6 can be filled by metal oxides and formed by removing the template.

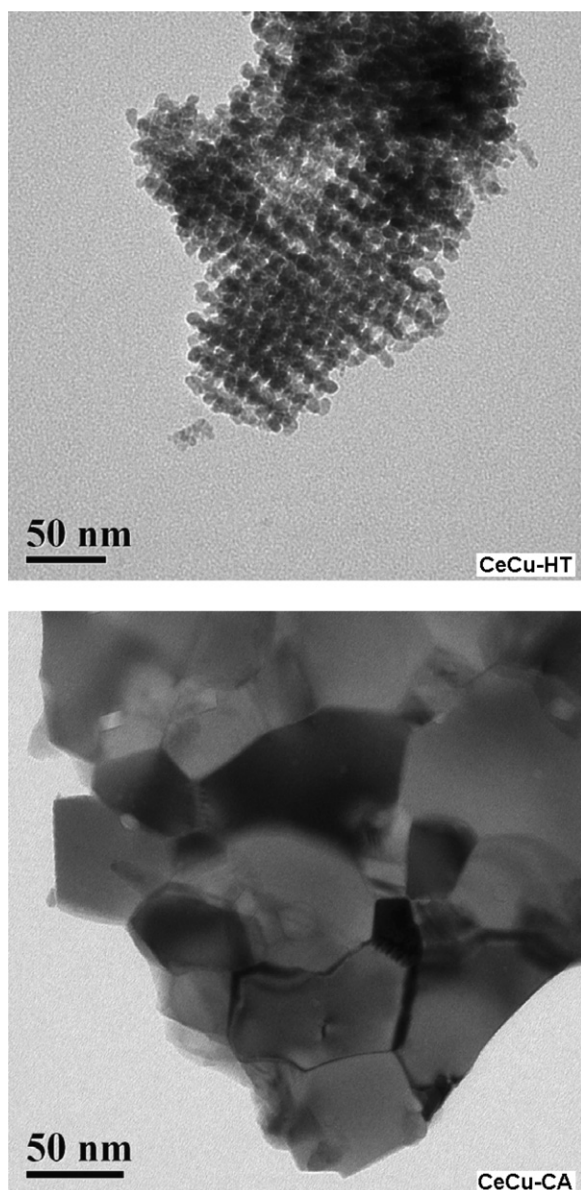


Fig. 2. TEM images of CeCu-HT and CeCu-CA catalysts.

Therefore, the porous structure of the prepared CeCu-HT catalyst can be attributed to the skeleton structure of KIT-6, whereas the skeleton structure of the prepared CeCu-HT catalyst can be attributed to the porous structure of the KIT-6 hard template. During catalyst preparation, the used KIT-6 template is vital to porous structure formation and pore size adjustment. The prepared CeCu-HT catalyst pore size can be directly affected by the skeleton structure size of the used template. The prepared CeCu-HT catalyst exhibits a developed porous structure, which can enhance the contact probability of catalysts with the reactant molecules. The porous structure can also result in an uneven surface force. These performances can improve the adsorption and activation of the reactant molecules on the prepared CeCu-HT catalyst. The prepared CeCu-CA catalyst does not develop a porous structure but forms a large aggregated structure. The surface force appears saturated. These factors are unfavorable to reactant adsorption and activation on the CeCu-CA catalyst. The surface active components and the interactions between components can generally be affected by the microscopic structure of a multicomponent composite oxide catalyst [20]. The catalytic performances can be affected by the surface active components and structural properties. Therefore, the catalytic activities of the prepared CeCu-HT and CeCu-CA catalysts clearly differ.

### 3.3. BET analysis

The nitrogen adsorption–desorption isotherms of the prepared CeCu-HT and CeCu-CA catalysts are shown in Fig. 3. The adsorption–desorption isotherm of the CeCu-HT catalyst is type IV based on the IUPAC classification [21]. Within a relatively low pressure range ( $P/P_0 < 0.55$ ), the adsorption of the sample is limited on a single molecular layer without hysteresis [22]. When  $P/P_0$  ranges from 0.55 to 0.75, the adsorption isotherm is convex shaped, indicating the high affinity of the adsorbates to

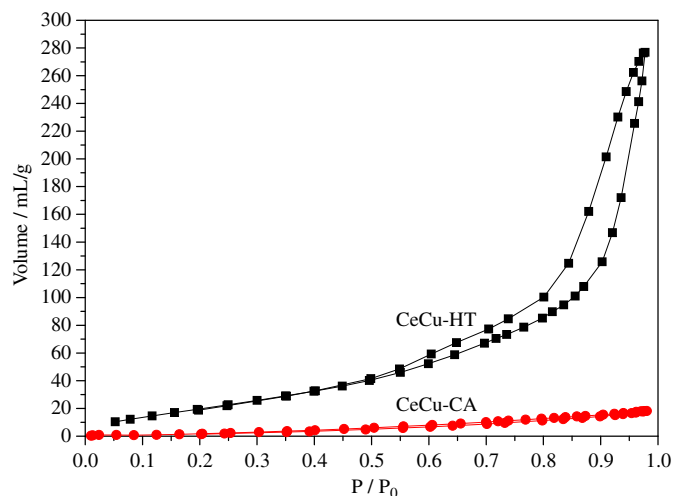


Fig. 3.  $N_2$  adsorption–desorption isotherms of CeCu-HT and CeCu-CA catalysts.



the CeCu-HT catalyst. When  $P/P_0$  ranges from 0.75 to 0.95, the adsorption isotherm shows a sudden, drastic change attributed to the capillary condensation as the adsorbance of the nitrogen molecules sharply increases [22]. At the same time, the  $N_2$  adsorption isotherm of the CeCu-HT catalyst does not coincide with the desorption isotherm. A type of H3 hysteresis loop also forms within the studied pressure range, which is mainly associated with the distinct porous structure of the catalyst [23]. Type IV adsorption is a typical characteristic of mesoporous transition metal oxide catalysts prepared by ordered mesoporous hard-templating methods [24–26] and is consistent with the TEM and low-angle XRD characterization results. The specific surface area of the CeCu-HT catalyst calculated by the BET equation is  $206.1 \text{ m}^2 \text{ g}^{-1}$ .

For the CeCu-CA catalyst, the  $N_2$  adsorption–desorption isotherms are almost straight lines and the  $N_2$  adsorption capacity is very low. When  $P/P_0$  exceeds 0.5, the  $N_2$  adsorbance does not exceed  $20 \text{ mL g}^{-1}$ . This result demonstrates that the catalyst has a very weak affinity with adsorbed gas molecules as well as a weak adsorption capacity for gas molecules. Gas molecules can be adsorbed by solid materials because of the uneven forces on the surface of solid materials. The low  $N_2$  adsorption capacity of the CeCu-CA catalyst can be attributed to the very small interface, low porosity, and rare uneven forces on the surface of the catalyst for  $N_2$  adsorption [22]. This result well agrees with the agglomerated structure from the TEM image. The specific surface area of the CeCu-CA catalyst calculated by the BET method is only  $23.5 \text{ m}^2 \text{ g}^{-1}$ . Therefore, the ordered mesoporous CeCu-HT composite oxide solid solution catalyst with a large specific surface area can be synthesized by hard templating. The ordered mesoporous structure and large specific surface area can enhance the adsorption capacity for the reactant molecules, which leads to improved catalytic properties [22,23].

### 3.4. Catalytic activity test

The CeCu-HT and CeCu-CA catalysts were prepared by hard-templating and complex methods at a Ce/Cu molar ratio of 3.0, respectively. The catalytic activity was evaluated by the catalytic combustion of 1.0% toluene (by volume) in air. The relationship between the reaction temperatures and the catalytic combustion conversion of toluene is shown in Fig. 4.

The CeCu-HT and CeCu-CA catalysts exhibit high catalytic combustion activity for toluene. However, the catalytic combustion activity of the CeCu-HT catalyst is higher than that of the CeCu-CA catalyst. During toluene catalytic combustion, the minimum reaction temperature at which toluene conversion exceeds 90% ( $T_{90}$ ) of the CeCu-HT catalyst is  $225^\circ\text{C}$ . The toluene removal rate exceeds 99.3% with decreased toluene concentration in air to below  $70 \text{ ppm}$  at  $240^\circ\text{C}$ . However, the  $T_{90}$  of the CeCu-CA catalyst reaches  $280^\circ\text{C}$ . The catalytic combustion conversion of toluene is only 72% even though the

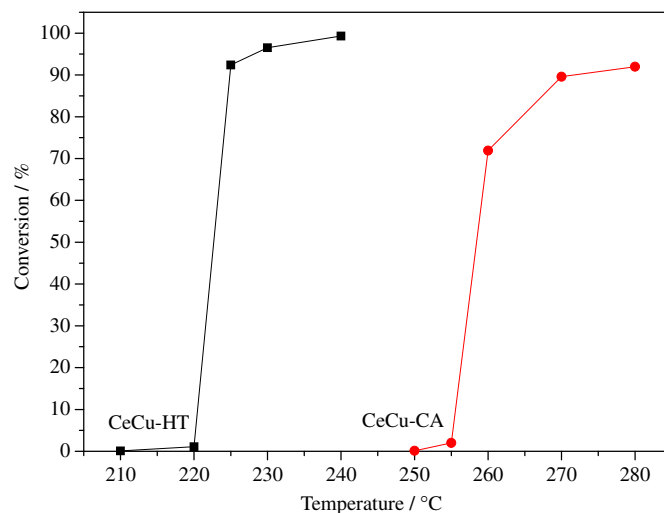


Fig. 4. Relationship between reaction temperature and toluene catalytic combustion conversion on CeCu-HT and CeCu-CA catalysts.

reaction temperature is  $260^\circ\text{C}$ . The catalytic combustion temperature of toluene is below  $300^\circ\text{C}$  over the CeCu-HT and CeCu-CA catalysts. The catalytic combustion activity for toluene over the CeCu-HT catalyst is clearly superior to that over the precious metal catalysts Pd [11] and Ru [12]. These results indicate that the CeCu-HT catalyst is a cheap and efficient catalyst that can be specifically used for the elimination of toluene from air.

The catalytic performance of catalysts in the combustion reaction of organic pollutants is a comprehensive property exhibited by the chemical composition and structure of the catalyst. The XRD results show that the  $\text{CeO}_2\text{--CuO}$  solid solution is the major component of the CeCu-HT and CeCu-CA catalysts. A small amount of the CuO phase is also present in the CeCu-CA catalyst. The CeCu-HT catalyst has a poor oxide crystalline phase structure, and negligible amounts of the CuO phase are detected. TEM and BET results reveal many differences between the CeCu-HT and CeCu-CA catalyst structures. The CeCu-HT catalyst has a developed ordered mesoporous structure and a large specific surface area of  $206.1 \text{ m}^2 \text{ g}^{-1}$ . On the other hand, the CeCu-CA catalyst has a massive structure with a specific surface area of only  $23.5 \text{ m}^2 \text{ g}^{-1}$ . The differences between the compositions and structures of the CeCu-HT and CeCu-CA catalysts may be the primary reason for their discrepant toluene catalytic combustion activities in air. The prepared CeCu-HT catalyst has high toluene catalytic combustion activity, which can be attributed to the developed ordered mesoporous structure and large specific surface area.

$\text{CeO}_2$  materials have high oxygen-storage and -release capacities. The mutual transformation of the  $\text{Ce}^{4+}/\text{Ce}^{3+}$  couple promotes the cycle of oxygen storage and release, which ensures that the catalyst surface has rich active oxygen species [27–31]. Thus, the CeCu-HT and CeCu-CA catalysts with  $\text{CeO}_2$  as the matrix show high toluene catalytic combustion activity in air. In the  $\text{CeO}_2\text{--CuO}$  solid solution, the  $\text{Cu}^{2+}$  species substitute for the

segmental  $\text{Ce}^{4+}$  species in the  $\text{CeO}_2$  crystal lattice to produce oxygen vacancies. Strong interactions are generated between the CuO and  $\text{CeO}_2$  species. The Cu–O and Ce–O bonds are weakened, which results in the fracturing of “metal–oxygen” bonds in appropriate reaction conditions to generate active oxygen species. Thus, the  $\text{CeO}_2$ –CuO solid solution displays higher reducibility than the  $\text{CeO}_2$  or CuO species. The catalytic oxidative activity of the  $\text{CeO}_2$ –CuO solid solution is also considerably higher than that of CuO or  $\text{CeO}_2$  [32]. During catalytic oxidation reaction, the adsorption and activation of  $\text{O}_2$  molecules benefit from the existence of weak “metal–oxygen” bonds, which can produce active oxygen species for the oxidation reaction to promote the toluene catalytic combustion reaction in air. The CeCu-HT catalyst has a higher toluene catalytic combustion activity than the CeCu-CA catalyst, which can be attributed to the complete dissolution of the CuO species in the  $\text{CeO}_2$  lattice to form the  $\text{CeO}_2$ –CuO solid solution. The interaction between  $\text{CeO}_2$  and CuO also significantly improves. On the other hand, the porous structure and large specific surface area of the CeCu-HT catalyst increase the catalyst adsorption capacity for gas reactant molecules. This finding is confirmed by the  $\text{N}_2$  adsorption–desorption isotherm results from the BET characterization. Therefore, the reactant molecules (e.g., toluene and  $\text{O}_2$  molecules) can be more easily adsorbed by the CeCu-HT catalyst than by the CeCu-CA catalyst. The catalyst has a high adsorption capacity for reactant molecules and can activate these reactant molecules, which results in enhanced catalytic properties. At the same time, the CeCu-HT catalyst has a larger specific surface area than the CeCu-CA catalyst. The increased contact area with the reactant molecules significantly improves the adsorption and activation abilities of the CeCu-HT catalyst. The prepared CeCu-HT catalyst with an ordered mesoporous structure significantly promotes the migration and diffusion of the reactant and product molecules onto the surface or into the porous CeCu-HT catalyst structure. Therefore, during the catalytic combustion of toluene in air, the superior composition and structure of the CeCu-HT catalyst are responsible for the higher catalytic activity of this catalyst than that of the CeCu-CA catalyst.

#### 4. Conclusions

Templating methods were successfully used to prepare composite oxide catalysts with a porous structure. The ordered mesoporous KIT-6 was used as the hard template to prepare a CeCu-HT catalyst with a large specific surface area of  $206.1 \text{ m}^2 \text{ g}^{-1}$  and an ordered mesoporous structure with an aperture of 5–6 nm. The CeCu-HT catalyst exhibits high metal-oxide dispersion and a uniform  $\text{CeO}_2$ –CuO solid solution phase. The CeCu-CA catalyst, which was prepared by the complex method, has a weakly porous structure and low specific surface area of  $23.5 \text{ m}^2 \text{ g}^{-1}$ . The CeCu-HT catalyst has higher toluene catalytic combustion activity in air than the CeCu-CA

catalyst.  $T_{90}$  of the catalytic combustion of toluene on the CeCu-HT catalyst is  $225^\circ\text{C}$ . The toluene catalytic combustion conversion exceeds 99.3% with decreased toluene concentration in air to below 70 ppm at  $240^\circ\text{C}$ . The catalytic combustion conversion of toluene is only 92% on the CeCu-CA catalyst even when the reaction temperature reaches  $280^\circ\text{C}$ . The differences between the toluene catalytic combustion performances of CeCu-HT and CeCu-CA can be attributed to their discrepant compositions and structures. The CeCu-HT catalyst, which has a large specific surface area and a developed ordered mesoporous structure, has high potential for toluene removal from air.

#### Acknowledgments

The work was financially supported by Natural Science Foundation Project of CQ CSTC (CSTC, 2011jjA2008); Key Fund of Chongqing Technology and Business University (No. 1252001); Fund of the State Key Laboratory of Catalysis in DICP (No. N-11-04); Program for Chongqing Innovative Research Team Development in University (KJTD201020).

#### References

- [1] S.A. Hosseini, A. Niaei, D. Salari, S.R. Nabavi, Nanocrystalline  $\text{AMn}_2\text{O}_4$  (A=Co, Ni, Cu) spinels for remediation of volatile organic compounds-synthesis, characterization and catalytic performance, *Ceramics International* 38 (2012) 1655–1661.
- [2] W.B. Li, J.X. Wang, H. Gong, Catalytic combustion of VOCs on non-noble metal catalysts, *Catalysis Today* 148 (2009) 81–87.
- [3] S.H. Taylor, C.S. Heneghan, G.J. Hutchings, I.D. Hudson, The activity and mechanism of uranium oxide catalysts for the oxidative destruction of volatile organic compounds, *Catalysis Today* 59 (2000) 249–259.
- [4] W.B. Li, W.B. Chu, M. Zhuang, J. Hua, Catalytic oxidation of toluene on Mn-containing mixed oxides prepared in reverse micro-emulsions, *Catalysis Today* 93–95 (2004) 205–209.
- [5] M.N. Padilla-Serrano, F.J. Maldonado-Hódar, C. Moreno-Castilla, Influence of Pt particle size on catalytic combustion of xylenes on carbon aerogel-supported Pt catalysts, *Applied Catalysis B* 61 (2005) 253–258.
- [6] H.S. Kim, T.W. Kim, H.L. Koh, S.H. Lee, B.R. Min, Complete benzene oxidation over Pt–Pd bimetal catalyst supported on  $\gamma$ -alumina: influence of Pt–Pd ratio on the catalytic activity, *Applied Catalysis A* 280 (2005) 125–131.
- [7] M.A. Centeno, M. Paulis, M. Montes, J.A. Odriozola, Catalytic combustion of volatile organic compounds on gold/titanium oxynitride catalysts, *Applied Catalysis B* 61 (2005) 177–183.
- [8] X.W. Su, L.Y. Jin, J.Q. Lu, M.F. Luo,  $\text{Pd/Ce}_{0.9}\text{Cu}_{0.1}\text{O}_{1.9}$ – $\text{Y}_2\text{O}_3$  catalysts for catalytic combustion of toluene and ethyl acetate, *Journal of Industrial and Engineering Chemistry* 15 (2009) 683–686.
- [9] S. Aouad, E. Abi-Aad, A. Aboukaïs, Simultaneous oxidation of carbon black and volatile organic compounds over Ru/ $\text{CeO}_2$  catalysts, *Applied Catalysis B* 88 (2009) 249–256.
- [10] T. Ataloglou, J. Vakros, K. Bourikas, C. Fountzoula, C. Kordulis, A. Lycourghiotis, Influence of the preparation method on the structure-activity of cobalt oxide catalysts supported on alumina for complete benzene oxidation, *Applied Catalysis B* 57 (2005) 299–312.

- [11] L.R. Gao, Y.N. Shen, K.B. Wang, Studies on  $\text{LaAlO}_3$  as a second support in the combustion catalyst, *Journal of Molecular Catalysis (China)* 16 (2002) 39–43.
- [12] J.G. Deng, L. Zhang, H.X. Dai, H. He, C.T. Au, Hydrothermally fabricated single-crystalline strontium-substituted lanthanum manganite microcubes for the catalytic combustion of toluene, *Journal of Molecular Catalysis A* 299 (2009) 60–67.
- [13] F. Jiao, A.H. Hill, A. Harrison, A. Berko, A.V. Chadwick, P.G. Bruce, Synthesis of ordered mesoporous  $\text{NiO}$  with crystalline walls and a bimodal pore size distribution, *Journal of the American Chemical Society* 130 (2008) 5262–5266.
- [14] J.K. Zhu, Q.M. Gao, Z. Chen, Preparation of mesoporous copper cerium bimetal oxides with high performance for catalytic oxidation of carbon monoxide, *Applied Catalysis B* 81 (2008) 236–243.
- [15] H. Tüysüz, M. Comotti, F. Schüth, Ordered mesoporous  $\text{Co}_3\text{O}_4$  as highly active catalyst for low temperature CO-oxidation, *Chemical Communications* 34 (2008) 4022–4024.
- [16] F. Kleitz, S.H. Choi, R. Ryoo, Cubic  $1a3d$  large mesoporous silica: synthesis and replication to platinum nanowires, carbon nanorods and carbon nanotubes, *Chemical Communications* 17 (2003) 2136–2137.
- [17] J. Rebellato, M.M. Natile, A. Glisenti, Influence of the synthesis procedure on the properties and reactivity of nanostructured ceria powders, *Applied Catalysis A* 339 (2008) 108–120.
- [18] W.G. Su, S.G. Wang, P.L. Ying, Z.C. Feng, C. Li, A molecular insight into propylene epoxidation on  $\text{Cu/SiO}_2$  catalysts using  $\text{O}_2$  as oxidant, *Journal of Catalysis* 268 (2009) 165–174.
- [19] G. Avgouropoulos, T. Ioannides, H. Matralis, Influence of the preparation method on the performance of  $\text{CuO-CeO}_2$  catalysts for the selective oxidation of CO, *Applied Catalysis B* 56 (2005) 87–93.
- [20] K. Soni, B.S. Rana, A.K. Sinha, A. Bhaumik, M. Nandi, M. Kumar, G.M. Dhar, 3-D ordered mesoporous KIT-6 support for effective hydrodesulfurization catalysts, *Applied Catalysis B* 90 (2009) 55–63.
- [21] K.S.W. Sing, D.H. Everett, R.A.W. Haul, L. Moscou, R.A. Pierotti, J. Rouquérol, Reporting physisorption data for gas/solid systems with special reference to the determination of surface area and porosity, *Pure and Applied Chemistry* 57 (1985) 603–619.
- [22] X.C. Fu, W.X. Shen, *Chinese Physical Chemistry [M]*, fourth edition, High education press, Beijing, 1990 943–947.
- [23] Z.Z. Gao, H.X. Dai, *Application Catalysis [M]*, second edition, Chemical industry press, Beijing, 2011 167–175.
- [24] F. Jiao, A. Harrison, J.C. Jumas, A.V. Chadwick, W. Kockelmann, P.G. Bruce, Ordered mesoporous  $\text{Fe}_2\text{O}_3$  with crystalline walls, *Journal of the American Chemical Society* 128 (2006) 5468–5474.
- [25] F. Jiao, J.C. Jumas, M. Womes, A.V. Chadwick, A. Harrison, P.G. Bruce, Synthesis of mesoporous  $\text{Fe}_3\text{O}_4$  and  $\gamma\text{-Fe}_2\text{O}_3$  with crystalline walls using post-template reduction/oxidation, *Journal of the American Chemical Society* 128 (2006) 12905–12909.
- [26] F. Jiao, A. Harrison, A.H. Hill, P.G. Bruce, Mesoporous  $\text{Mn}_2\text{O}_3$  and  $\text{Mn}_3\text{O}_4$  with crystalline walls, *Advanced Materials* 19 (2007) 4063–4066.
- [27] G. Balducci, M.S. Islam, J. Kašpar, P. Fornasiero, M. Graziani, Bulk reduction and oxygen migration in the Ceria-based oxides, *Chemistry of Materials* 12 (2000) 677–681.
- [28] B.M. Reddy, P. Lakshmanan, A. Khan, Investigation of surface structures of dispersed  $\text{V}_2\text{O}_5$  on  $\text{CeO}_2\text{-SiO}_2$ ,  $\text{CeO}_2\text{-TiO}_2$ , and  $\text{CeO}_2\text{-ZrO}_2$  mixed oxides by XRD, raman, and XPS techniques, *The Journal of Physical Chemistry B* 108 (2004) 16855–16863.
- [29] B.M. Reddy, P. Bharali, P. Saikia, G. Thrimurthulu, Y. Yamada, T. Kobayashi, Thermal stability and dispersion behavior of nanostructured  $\text{Ce}_x\text{Zr}_{1-x}\text{O}_2$  mixed oxides over anatase- $\text{TiO}_2$ : a combined study of CO oxidation and characterization by XRD, XPS, TPR, HREM, and UV Vis-DRS, *Industrial & Engineering Chemistry Research* 48 (2009) 453–462.
- [30] N. Hickey, P. Fornasiero, R. DiMonte, J. Kaspar, M. Graziani, G. Dolcetti, A comparative study of oxygen storage capacity over  $\text{Ce}_{0.6}\text{Zr}_{0.4}\text{O}_2$  mixed oxides investigated by temperature-programmed reduction and dynamic OSC measurements, *Catalysis Letters* 72 (2001) 45–50.
- [31] S.N. Achary, S.K. Sali, N.K. Kulkarni, P.S.R. Krishna, A.B. Shinde, A.K. Tyagi, Intercalation/deintercalation of oxygen: a sequential evolution of phases in  $\text{Ce}_2\text{O}_3/\text{CeO}_2\text{-ZrO}_2$  pyrochlores, *Chemistry of Materials* 21 (2009) 5848–5859.
- [32] F.X. Yin, S.F. Ji, N.Z. Chen, L.P. Zhao, W. Wang, C.Y. Li, H. Liu, Catalytic combustion of methane over  $\text{Ce}_{1-x}\text{Cu}_x\text{O}_{2-x}/\text{Al}_2\text{O}_3$  solid solution catalyst, *Journal of Chemical Industry and Engineering (China)* 57 (2006) 744–750.